Relating Statistical MOSFET Model Parameter Variabilities to IC Manufacturing Process Fluctuations Enabling Realistic Worst Case Design

James A. Power, *Member, IEEE,* Brian Donnellan, Alan Mathewson, and William A. Lane

Abstract— The implementation of a viable statistical circuit design methodology requiring detailed knowledge of the variabilities of, and correlations among, the circuit simulator model parameters utilized by designers, and the determination of the important relationships between these CAD model parameter variabilities and the process variabilities causing them is presented. This work addresses the above requirements by detailing a new framework which was adopted for a 2-μm CMOS technology to enable realistic statistical circuit performance prediction prior to manufacture. Issues relating to MOSFET modeling, the derivation of fast "direct" parameter extraction methodologies suitable for rapid parameter generation, the employment of multivariate statistical techniques to analyze statistical parametric data, and the linking of the CAD model parameter variations to variabilities in process quantities are discussed. In this approach the correlated set of model parameters is reduced to a smaller and more manageable set of uncorrelated process-related factors. The ensuing construction and validation of realistic statistical circuit performance procedures is also discussed. Comparisons between measured and simulated variabilities of device characteristics is utilized to demonstrate the accuracy of the techniques described. The advantages of the proposed approach over more traditional "worst case" design methodologies are demonstrated.

I. INTRODUCTION

THE semiconductor industry is constantly striving to optimize profits by increasing product yield and reliability while decreasing product development time and cost. Central to the achievement of these aims is the necessity to initiate so-called design for manufacturability (DFM) [1] efforts. An integral component of any DFM activity entails the prediction, prior to manufacture, of both nominal circuit behavior and the expected process-induced statistical circuit performance spreads. Reported methodologies which can be used to predict statistical circuit performance spreads have been many and varied [2]–[8]. Some such methodologies, on which this work is based, involve statistical multivariate analyses of measured model parameter information gathered over a period of time from a relatively stable manufacturing process. These approaches have the advantage of being based on the analysis of the very parameters which the designers will use in circuit simulation. The model parameters are

relatively easy to extract and some may already be routinely recorded as part of the existing in-line process monitor tests. In addition, most if not all of the parameters can be extracted from standard parameter extraction test structures consisting of devices with a variety of drawn dimensions. Manipulation of this type of parametric data can enable the accurate and efficient prediction of device and circuit performance spreads which occur as a direct consequence of inevitable process disturbances. Ideally, in these schemes the measured correlated model parameter set is transformed into a much smaller and more workable set of independent factors either by a principal component analysis [6], [9]–[12] or by some related factor analysis [7]. Circuit simulation frameworks utilizing these factors and either a Monte Carlo analysis [6], gradient analysis [7], [13], or simply some worst case methodology will enable the accurate prediction of the required statistical circuit performance spreads.

The accuracy of the circuit simulator device model and of its companion parameter extraction techniques is central to the feasibility of any circuit performance prediction methodologies. If the model is being utilized to simulate analog circuits then it should be capable of adequately predicting device conductances as well as currents in all regions of device operation especially at low gate drives [14], [15]. Parameter extraction techniques for this model should be both accurate and efficient. Accurate model parameters will ensure that the best use is made of the model but the efficiency of the parameter extractions is also a major consideration for the purposes of gathering statistical parametric data in large quantities. Traditional parameter extraction procedures which employ optimization techniques [16]–[18] are certainly accurate but they are too time consuming and CPU-intensive to be practical for the proposed task. Parameter optimization may also introduce artificial correlations between the extracted model parameters. A more suitable means of acquiring parameter values is by the use of so-called "direct" parameter extraction methods [19]–[21] utilizing analytical equation solving techniques formulated specifically for the model in use.

The independent factors obtained from the analysis of device model parameters can be related to some underlying process fluctuations. It will be shown in this work that it is possible to identify the most significant process disturbances (i.e., variations in oxide thickness, line-width and doping) which are instrumental in causing specific MOSFET model

parameter variabilities and correlations. The subsequent definition of relationships between the original model parameters, which are often empirical in nature, and the more physical process related quantities, forges an invaluable link between circuit design and process technology tasks. Specific critical model parameter variabilities can be traced back to process parameter fluctuations and it then becomes possible to improve circuit yield by tightening the controls of the process variables isolated. Furthermore, the process-related factors can be derived much more easily than the process variables themselves can be measured and this simplifies the task of monitoring the process.

This paper describes the acquisition and statistical analysis of MOSFET model parametric information using as an example a 2-μm CMOS process and also suggests some methods by which the data obtained can be utilized to predict statistical device and circuit performance variabilities. The MOSFET model employed during this work will be detailed in Section II along with its dedicated direct parameter extraction techniques. The analysis of the measured parametric data using a principal component analysis based technique and the derivation of relationships between model and process parameters will be summarized in Section III. In Section IV various statistical and worst case circuit design procedures will be proposed and measured device performance variations will be utilized to validate them. Section V contains a summary and conclusions.

II. MODEL AND PARAMETER EXTRACTION

The first stage in successful parametric yield modeling must be the selection of a suitable MOSFET model and the subsequent definition of parameter extraction schemes appropriate for the collection of large amounts of parametric data as part of in-line process monitor tests. The model equations utilized were based on a previously published model [22] with certain modifications to allow accurate predictions of device transconductance, output conductance, substrate bias effects, and subthreshold behavior. Techniques for the extraction of model parameters via optimization alogrithms were implemented and employed for model validation purposes.

However, this parameter extraction procedure with its large measurement requirements, its CPU demands, and the sheer amount of time involved was not suitable for inclusion into any in-line process monitor test framework. In order to achieve parameter extraction in a form appropriate for our application direct parameter extraction strategies were utilized. Direct parameter extraction requires the measurement of a minimized data set and the generation of parameter values via analytical equation solving techniques formulated for the particular model in use. Direct parameter extraction techniques are fast, accurate, and minimize instances of parameter extraction induced correlations as well as preventing parameters attaining unrealistic or unphysical values. These problems are a characteristic feature of parameter optimization techniques where parameters which have similar influence on device characteristics can interact or a parameter may be optimized to data measured in a region of operation in which it should have no relevance. Direct parameter extraction methodologies are however not as versatile as their optimization counterparts because knowledge of the model equations is inherently inbuilt into the procedures and model equation changes normally require significant reworking of these procedures.

A. Model Equations

The following are the MOSFET model equations for predicting strong-inversion currents. The implementation of subthreshold current is virtually the same as the BSIM1 [23] model. Table I lists and describes the relevant model parameters. In the strong-inversion region of operation

$$I_{DS} = \text{UO} \times Fg \times Fm \times COX \times \frac{W}{L}$$
$$\times Fv \times Fq \times V_{DSX} \tag{1}$$

where the low-field mobility (UO) has units cm^2/(V · s) and the effective dimensions are given by

$$W = W\text{drawn} + \text{DW} \tag{2}$$
$$L = L\text{drawn} - 2 \times \text{LD}. \tag{3}$$

In (1),

$$Fg = \frac{1}{1 + \text{THETA} \times (V_{GS} - \pm\text{VFB}) + \text{TH2} \times \frac{V_{DS}}{L} + \text{THETA}B \times \text{GAMMA} \times (\sqrt{\text{PHI} - V_{BS}} - \sqrt{\text{PHI}})} \tag{4}$$

$$Fm = 1 + \text{LAMBDA} \times \left(\sqrt{V_{DS} + \text{GG}^2} - \text{GG} \right) \tag{5}$$

$$Fv = \frac{1}{1 + \dfrac{V_{DSX} \times \text{UO} \times Fg \times Fm}{\text{VMAX} \times L}} \tag{6}$$

and

$$Fq = V_{GS} - VON - \left(1 + \frac{\text{GAMMA}}{4 \times \sqrt{\text{PHI} - V_{BS}}} \right) \times \frac{V_{DSX}}{2}. \tag{7}$$

TABLE I
MOSFET MODEL PARAMETERS

Name	Comment	Units
VFB	Flat-band voltage	V
GAMMA	Bulk threshold parameter	$V^{1/2}$
PHI	Surface Potential	V
LAMBDA	Channel length modulation	V^{-1}
TOX	Oxide thickness	m
UO	Surface mobility	cm^2/Vs
VMAX	Maximum carrier drift velocity	m/s
THETA	Mobility modulation	V^{-1}
THETAB	Body effect mobility parameter	V^{-1}
GA2	Linear GAMMA parameter	—
TH2	V_{DS} dependent mobility term	m/v
SIGMA	Static drain feedback	—
SIGMAB	Body effect static drain feedback	V^{-1}
GG	Output conductance parameter	—
N0	Zero bias gate drive coefficient	—
ND0	V_{DS} bias gate drive coefficient	V^{-1}
NB0	V_{BS} bias gate drive coefficient	V^{-1}
NC	Weak inversion fitting parameter	—
LD	Channel length reduction parameter	μm
DW	Channel width reduction parameter	μm
RSH	Drain/source resistance parameter	Ω/sq

The threshold voltage is given by the expression

$$VON = VTO + GAMMA$$
$$\times (\sqrt{PHI - V_{BS}} - \sqrt{PHI}) - GA2$$
$$\times (PHI - V_{BS}) - f(V_{DS}) \qquad (8)$$

where

$$f(V_{DS}) = SIGMA \times V_{DS}$$
$$\times (1 + SIGMAB \times GAMMA$$
$$\times (\sqrt{PHI - V_{BS}} - \sqrt{PHI})) \qquad (9)$$

and

$$VTO = \pm VFB + PHI + GAMMA \times \sqrt{PHI}. \qquad (10)$$

The saturation voltage is

$$VSAT = \frac{VMAX \times L}{UO \times Fg \times Fm}$$
$$\times \left(\sqrt{1 + \frac{2 \times (V_{GS} - VON)}{\frac{VMAX \times L}{UO \times Fg \times Fm} \times \left(1 + \frac{GAMMA}{4 \times \sqrt{PHI - V_{BS}}}\right)}} - 1 \right) \qquad (11)$$

and

$$V_{DSX} = \min(V_{DS}, VSAT). \qquad (12)$$

In (4) and (10) the plus sign corresponds to n-channel devices and the minus sign corresponds to p-channel devices. These equations were found to be adequate for modeling devices from the 2-μm CMOS process used during this work. Further model enhancements were necessary, especially in saturation region modeling, to accurately characterize devices from a 1-μm technology which has since been developed.

B. Parameter Extraction

Direct parameter extraction is not always an easy task. Problems can arise where the model equations are complicated and/or where it is impossible to decouple certain parameters which characterize similar effects. Care should be exercised during the formulation of a model so as to ensure that fast noniterative forms of parameter extraction are possible. This does not always happen and the effects of individual model parameters cannot always be separated from each other. In the case of the model employed in this work the direct extraction of linear, subthreshold, and certain saturation region parameters was relatively straight forward. Difficulties were encountered in the extraction of the remaining saturation region parameters and steps had to be taken to simplify the task. For the devices under analysis it was found, using parameter optimization, that setting the TH2 parameter to zero did not significantly affect the model's performance. Similarly it was determined that the parameter GG could be set to predefined values of 0.5 for n-channel devices and 1.0 for p-channel devices. In addition, the parameters PHI and TOX were held at process dependent values during the extractions.

The following is an example of the methodology used to extract model parameters in a direct fashion. In the linear region of operation at low drain-source biases the current equation can be simplified to become

$$I_{DS} = \frac{\beta \times V_{DS}}{THETA}$$
$$\times \frac{V_{GS} - \left(VON + \frac{V_{DS}}{2}\right)}{V_{GS} - \left(\pm VFB - \frac{1}{THETA}\right)}. \qquad (13)$$

Expression (13) can be written in a more general form as [19], [21]

$$I_{DSn} = Z_n = \frac{a \times (X_n - b)}{(Y_n - c)} \qquad n = 1, 2, 3 \qquad (14)$$

where $X_n = Y_n = V_{GSn}$ and with

$$a = \frac{\beta \times V_{DS}}{THETA} = \frac{UO \times COX \times W}{L} \times \frac{V_{DS}}{THETA} \qquad (15)$$

$$b = VON + \frac{V_{DS}}{2} \qquad (16)$$

and

$$c = \pm VFB - \frac{1}{THETA}. \qquad (17)$$

Thus, three measurements of device current (I_{DS}) at three specially chosen biases (V_{GS}) in the linear region of device operation can be used in solving three equations in three unknowns to yield values for $a, b,$ and c. This is repeated for three substrate biases nominally 0.0 V, $-/+2.5$ V, and

$-/+5$ V. A typical biasing arrangement is shown below

$$V_{GS1} = VON_{approx} \pm 0.4V$$

$$V_{GS2} = V_{GS1} + \frac{V_{GMAX} - V_{GS1}}{4}$$

$$V_{GS3} = V_{GSMAX}. \tag{18}$$

In (18) V_{GSMAX} is usually $+/-5$ V. Threshold voltages (VON's) are calculated from (16) and values of b at the three chosen substrate biases. Expressions (8) and (10) are then solved to calculate VFB, GAMMA, and GA2 parameters. The parameters THETA and UO, for each substrate bias, are next extracted from the previously calculated c and a values using (17) and (15), respectively. These parameters in turn enable the calculation of the THETAB parameter. Thus, for a single device, 9 measurements of device current are sufficient to extract the VFB, GAMMA, GA2, UO, THETA, and THETAB parameters in a direct fashion.

In the next stage of the direct extraction process the parameters LD and DW, in addition to a value for the drain and souce parasitic resistance parameter RSH (units ohms per square), are determined from UO and THETA values extracted from devices with different geometries [21]. A minimum of three devices must be involved in this case, with drawn geometries of 20/20 μm, 20/2 μm, and 4/20 μm forming this minimum set. Similarly, direct methods are utilized to extract the N0, NB0, ND0, NC, SIGMA, and SIGMAB parameters from 8 current measurements in the weak-inversion region of operation. A further three measurements of current in the saturation region of operation form the basis for completing the parameter extraction by determining the VMAX and LAMBDA parameters. Table II details the entire direct parameter extraction process as performed in this work. Fig. 1 shows plots of measured and modeled $I-V$ curves for p-channel and n-channel 20/2 μm devices where the model parameters were extracted using the direct parameter extraction techniques described in this section. These plots also include the data points which were measured as part of the quick (direct) extraction procedure. The agreement between measured and modeled data is quite reasonable even at very low gate drives with the mean error between measured and simulated device currents rarely exceeding 5%, thus validating the use of the direct extraction methodology. Both the measurement of the data required for the direct parameter extractions and the extractions themselves for five n-channel and five p-channel devices took less than 1 min on the parametric test system on which the software was installed.

III. STATISTICAL PARAMETER ANALYSIS

The parameter extraction methodologies described in the previous section were employed to extract MOSFET model parameter sets over some specially fabricated wafers. Rather than build up a collection of parameter sets over a period of time from the process under investigation, it was decided to extract the required model parameters from a set of wafers which were fabricated under conditions where selected process input variables were intentionally perturbed within the extremes of their expected limits. Some of the

TABLE II
MOSFET DIRECT PARAMETER EXTRACTION SEQUENCE

Stage Number	Number of Measurements per Device	Parameters	Input	Region of Operation
1	9	VFB, UO(W,L), THETA(L), GAMMA, GA2, THETAB	$I-V$ Data	Linear
2	0	LD, DW, UO	UO(W, L)	Linear
3	0	RSH, THETA	THETA(L), UO	Linear
4	8	NC, N0, NB0, ND0, SIGMA, SIGMAB	$I-V$ Data	Subthreshold
5	3	VMAX, LAMBDA	$I-V$ Data	Saturation

process inputs which were varied included gate oxidation temperature, poly CD (polysilicon linewidth), N-well implant dose, P-well implant dose, threshold voltage adjust implant dose, N+ and P+ source/drain implant dose, and well drive-in temperature. In all, over 800 complete model parameter sets were measured, corresponding to the different process splits or perturbations. Similar results to those achieved from these wafers would be expected from the analysis of parametric data measured, for example, over a 6-monthly period from the same manufacturing process without intentional process variations being introduced.

A. Methodology

The measured parameter sets were then screened and any outliers in the data were eliminated. In the approach utilized here, parameters outside of their valid acceptable limits were first excluded and next parameter sets containing any parameter value outside of its $+/-4\sigma$ bounds were also deleted. This brought the number of remaining parameter sets in this example to just over 700. Parametric information, including parameter means, medians, variances, and distribution types were next determined. In the case of the MOSFET model parameters investigated, most of the distributions were either Gaussian or could be easily transformed so that they could be represented by Gaussian distributions. For example, some of the subthreshold parameters exhibited log-normal distributions and were transformed. Measured histograms of the low-field mobility parameter (UO) and flat-band voltage parameter (VFB) are shown in Fig. 2. These distributions are, for all practical purposes, Gaussian. Measured parameter means and standard deviations for n-channel and p-channel parameters for the 20/20 μm device are listed in Table III where the RSH parameter has been converted into an RDS parameter with units of ohms.

Accurate statistical circuit design or worst case design techniques can be quite difficult to implement if they are derived in terms of the model parameters. Inaccuracies usually occur as a direct consequence of the model parameters being treated as independent quantities in the interest of simplicity. Measured model parameters from most circuit simulator models, especially models of an empirical or semi-empirical nature, can be correlated with each other and in many cases
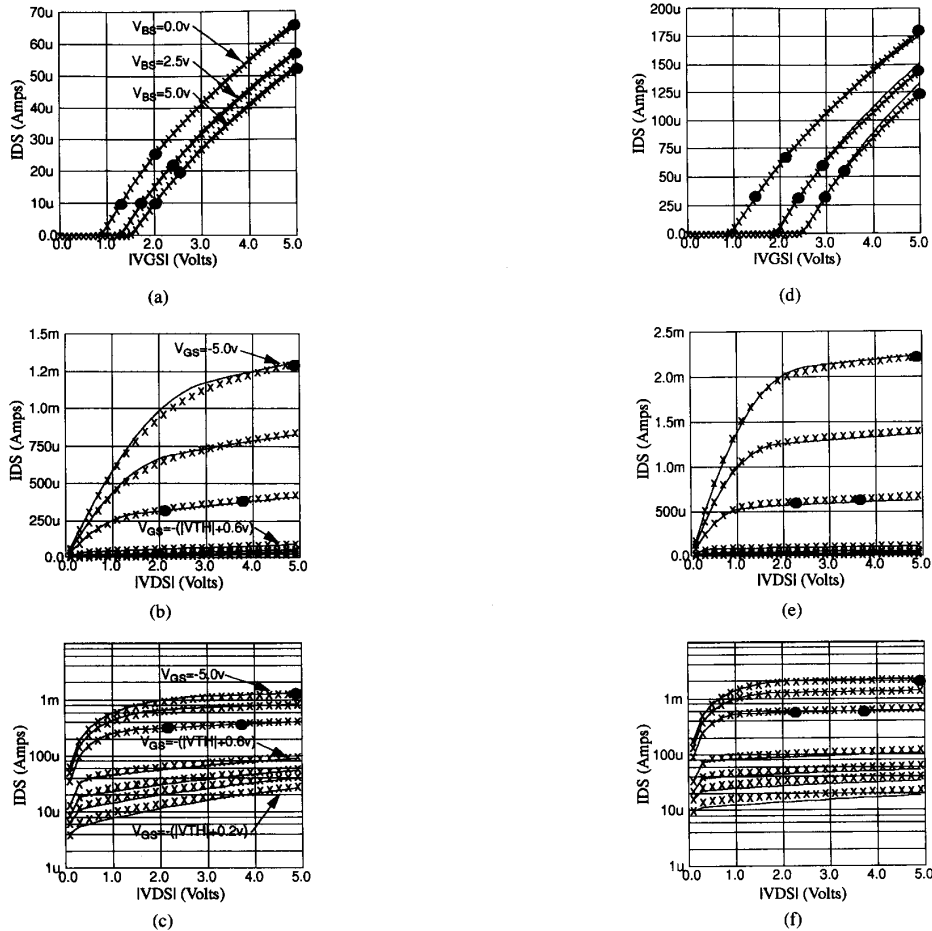
Fig. 1.   Measured (xxx) and simulated (——) characteristics for 20/2-μm p-channel and n-channel devices. (a), (b), (c) p-channel devices. (d), (e), (f) n-channel devices. Data utilized in direct parameter extractions is shown by the full circles.

highly correlated. Fig. 3 contains a scatter plot of measured VMAX and LAMBDA parameters for the 20/2-μm n-channel device. The parameters are negatively correlated having a correlation coefficient of -0.82. In the compilation of a worst case model parameter set, based only on setting worst case parameter limits in order to maximize device current or output conductance, one would be tempted to couple a high value of LAMBDA with a high value of VMAX. This situation is unlikely to occur as can be seen in the scatter plot. Many such situations can occur in the construction of worst case parameter sets because of the complicated interdependencies which can exist between model parameters. Ignoring parameter correlations usually results in worst case parameter sets leading to over pessimistic circuit performance spreads [10] which may in turn overcomplicate the circuit design procedure or wrongly suggest that a valid design could operate outside some of its performance specification limits.

In this work we employ a multivariate statistical technique called principal component analysis (PCA [24]) to examine the relationship between a set of n correlated parameters $(P_1, P_2, \cdots, P_n)$. PCA can effectively transform any set of parameters, and the complex relationships which exist between them, into a much more manageable set of uncorrelated quantities called principal components. The number of principal components (m) generally required to adequately represent a set of correlated parameters is much less than the original number of parameters which existed in the first place (i.e., $m \ll n$), thus making the principal components substantially easier to manipulate. The mathematical details associated with the derivation of the principal components are provided elsewhere [9], [10], and [24]. Additionally we have found it necessary to further transform the selected principal components into a set of rotated components or factors (X's) using a VARIMAX [25] orthogonal rotation. This is done because we have found that the rotated components prove to be easier to interpret than the principal components. Using this scheme any model parameter can now be expressed as a linear combination of the independent components

$$P_i = \sum_{j=1}^{m} a_{ij} X_j,$$

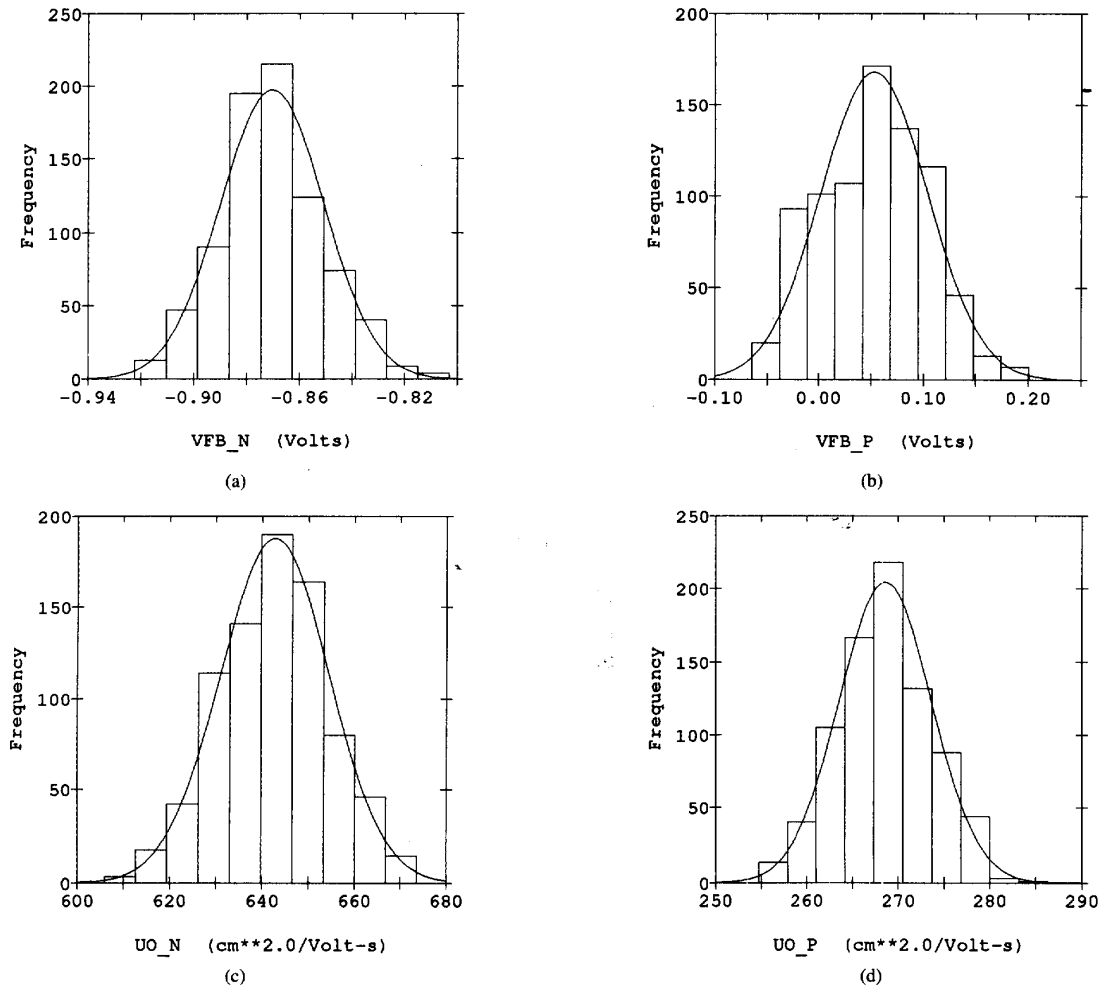$$i = 1 \text{ to } n \text{ where } m \ll n \qquad (19)$$

Fig. 2. Measured distributions of n-channel flat-band voltage parameter VFB. (a) p-channel VFB parameter. (b) n-channel low-field mobility parameter UO. (c) p-channel UO parameter.

where both the components and the parameters have been normalized to have a mean of zero and unit standard deviation. In (19) the a_{ij} coefficients are actually the correlation coefficients between the model parameters and the transformed components. These coefficients lie in the range -1 to $+1$ and are derived from the combination of PCA and VARIMAX transformations. An a_{ij} value with a magnitude close to unity implies a significant relationship between parameter P_i and component X_j while the opposite applies if a_{ij} is close to zero. The purpose of the VARIMAX transformation was to force all of the a_{ij} coefficients as close as possible to $+/-1$ or 0 so as to facilitate the interpretation of the components. By inverting the matrix of a_{ij} values as they appear in (19) expressions can be derived by which component values can be derived from any set of parameters.

B. Interpretation of Factors

Intuitively, the independent components should be related to the process steps or parameters whose variabilities are the root causes of the model parameter variations and cor-relations. Using a combination of information concerning the process settings under which the test wafers were fabricated, process monitor data gathered from these same wafers, and knowledge of the theoretical physical basis for the device model parameters, we hoped to identify the individual independent components as soon as they were derived. The analysis described above was performed on a set of parameters gathered from devices with a drawn width of 20 μm and drawn lengths of 2 μm, 4 μm, and 8 μm. For simplicity and without compromising model accuracy noticeably, the parameters THETAB, SIGMAB, and NB0 were eliminated from the analysis by being set to their mean measured values. The oxide thickness parameter (TOX) was added to the experiment by setting it to a nominal measured value for each programmed value of gate oxidation temperature. In all, the total combined parameter set contained 75 parameters (i.e., $n = 75$). The parameter set contained 25 CMOS parameters for each device geometry containing 12 n-channel parameters, 12 p-channel parameters, and a TOX parameter. The remaining 8 model parameters for each polarity were effectively eliminated from

TABLE III
MEASURED PARAMETER MEANS AND
STANDARD DEVIATIONS FOR 20/2-μm DEVICES

Parameter	Mean	Standard Deviation	Units
THETAB_N	−0.0890	0.0072	V^{-1}
GAMMA_N	1.1867	0.0778	$V^{1/2}$
GA2_N	0.0558	0.0102	—
VFB_N	−0.8704	0.0196	V
SIGMA_N	0.0103	0.0025	—
SIGMAB_N	1.8262	0.2566	V^{-1}
N0_N	1.8125	0.0506	—
NB0_N	0.1491	0.0209	V^{-1}
VMAX_N	152311	3202	m/s
LAMBDA_N	0.1871	0.0144	V^{-1}
RDS_N	75.0	7.4	Ω
THETA_N	0.0625	0.0019	V^{-1}
LD_N	0.4111	0.0454	μm
DW_N	−0.0351	0.0690	μm
UO_N	642.7	11.7	cm^2/Vs
THETAB_P	0.1683	0.0138	V^{-1}
GAMMA_P	0.4264	0.0240	$V^{1/2}$
GA2_P	0.0108	0.0038	—
VFB_P	0.0529	0.0511	V
SIGMA_P	0.0510	0.0093	—
SIGMAB_P	0.0844	0.1801	V^{-1}
N0_P	1.6141	0.0577	—
NB0_P	0.1123	0.0258	V^{-1}
VMAX_P	96827	17878	m/s
LAMBDA_P	0.4936	0.1500	V^{-1}
RDS_P	147.8	14.2	Ω
THETA_P	0.1260	0.0050	V^{-1}
LD_P	0.3964	0.0455	μm
DW_P	−0.0779	0.0603	μm
UO_P	268.6	5.0	cm^2/Vs

Fig. 4. General PCA and VARIMAX transformation framework.

rotations in order to calculate the required a_{ij} coefficients. A graphical representation of the transformation process as it refers to this example is shown in Fig. 4. Table IV lists these coefficients for the 20/2-μm device only. The individual parameter variances accounted for as a result of utilizing the 7 rotated components are also included in this table. The percentage variances attributed to each of these components, indicating their relative importance, are also given.

Scatter plots of the 4 most important rotated components versus parameters with which they are strongly correlated are shown in Fig. 5. Component $X_1, X_2, X_3, X_4, X_5, X_6,$ and X_7 are strongly related to the n-channel GAMMA body effect parameters, the channel length reduction parameters (LD's), p-channel flat-band voltage parameters (VFB's), n-channel low-field mobility parameters (UO's), channel width reduction parameters (DW's), n-channel flat-band voltage parameters, and n-channel drain/source parasitic resistance parameters (RDS's) respectively. As was previously mentioned, the components are normalized to have zero mean and unit standard deviation and component scores for each parameter set were obtained by inverting the system of equations given in (19). As an example the following expressions can now be written for the normalized n-channel THETA parameter and the normalized p-channel LAMBDA parameter associated with the 20/2-μm device.

THETA_N_norm

$$= 0.64X_1 - 0.03X_2 - 0.03X_3 + 0.57X_4$$
$$- 0.20X_5 - 0.05X_6 - 0.23X_7 \qquad (20)$$

LAMBDA_P_norm

$$= -0.48X_1 - 0.27X_2 + 0.67X_3 + 0.17X_4$$
$$+ 0.07X_5 - 0.06X_6 - 0.13X_7. \qquad (21)$$

By investigating scatter plots (e.g., Fig. 5), and by examining main effect plots such as those in Fig. 6, the 7 components were identified as being due to variations in gate oxide thickness ($X_1 = -X_{\Delta TOX}$), channel length reduction ($X_2 = -X_{\Delta L}$), threshold voltage adjust implant ($X_3 = -X_{\Delta VT}$), P-well implant ($X_4 = -X_{\Delta PWELL}$), channel width reduction ($X_5 = X_{\Delta W}$), n-channel flat-band voltage ($X_6 = X_{\Delta VFBN}$), and drain/source junction depth ($X_7 = X_{\Delta XJ}$). Fig. 6(a) is a plot showing X_1 averaged over certain wafers where the gate oxidation temperature (and thus gate oxide thickness)
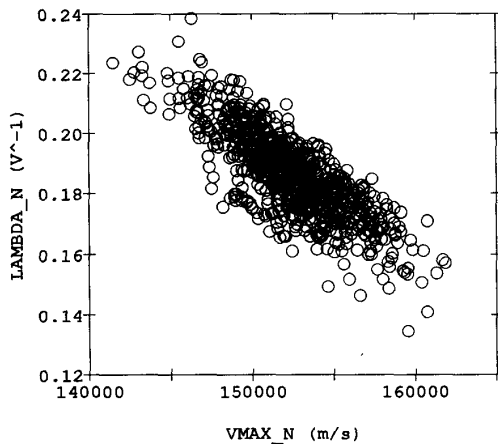

Fig. 3. Scatter plot of n-channel VMAX and LAMBDA parameters ($\rho = -0.85$).

the analysis by setting them to default values as mentioned above and in Section II. A PCA analysis of the parameter correlation matrix (R) determined that almost 81% of the variance of the 75 model parameters was accounted for by the first 7 principal components. These principal components were retained ($m = 7$) and subjected to VARIMAX orthogonal
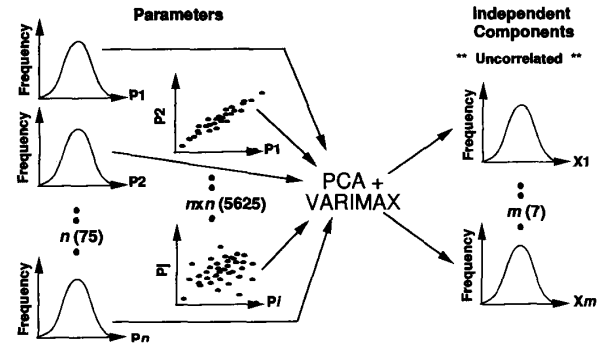
TABLE IV
THE a_{ij} COMPONENT SCORES FOR THE 20/2-μm DEVICES

Parameter	X_1 (29.1%)	X_2 (13.3%)	X_3 (14.9%)	X_4 (6.1%)	X_5 (7.6%)	X_6(4.1%)	X_7 (5.5%)	Variance
GAMMA_N	−0.95	0.16	0.00	−0.10	0.12	−0.09	0.01	96.2%
GA2_N	0.34	−0.69	−0.20	0.20	−0.01	−0.15	0.23	75.1%
VFB_N	0.42	−0.45	−0.06	0.09	−0.00	0.64	0.152	82.6%
SIGMA_N	0.04	−0.83	0.03	0.06	−0.05	−0.11	0.18	74.5%
N0_N	−0.97	0.09	0.04	−0.07	0.11	−0.05	0.05	96.7%
VMAX_N	−0.01	0.32	−0.10	0.00	−0.01	−0.08	−0.63	51.8%
LAMBDA_N	−0.05	−0.52	0.03	0.33	0.03	−0.07	0.52	66.1%
RDS_N;	−0.38;	0.11	0.13	−0.36	0.28	−0.10	0.72	80.5%
THETA_N	0.64	−0.03	−0.03	0.57	−0.20	−0.05	−0.23	81.5%
LD_N	0.13	−0.95	0.06	−0.08	−0.13	0.00	−0.03	94.2%
DW_N	0.11	0.03	−0.10	−0.05	−0.93	−0.07	−0.00	89.2%
UO_N	0.20	0.43	0.06	0.72	0.05	0.15	−0.01	77.4%
GAMMA_P	−0.75	0.54	0.13	−0.00	0.03	−0.04	0.10	88.2%
GA2_P	0.59	−0.03	−0.45	−0.12	−0.06	0.23	−0.14	63.4%
VFB_P	0.20	0.10	−0.93	−0.05	−0.13	0.15	−0.01	95.6%
SIGMA_P	0.08	−0.86	−0.40	0.08	0.02	0.10	−0.08	92.3%
N0_P	−0.18	−0.50	−0.71	0.07	−0.05	0.10	−0.02	79.5%
VMAX_P	0.47	0.17	−0.73	−0.17	−0.07	0.14	0.10	85.2%
LAMBDA_P	−0.48	−0.27	0.67	0.17	0.07	−0.06	−0.13	80.8%
RDS_P	−0.62	0.22	0.40	−0.01	0.17	−0.12	0.47	85.3%
THETA_P	0.78	−0.10	−0.53	−0.16	−0.10	−0.02	−0.18	96.0%
LD_P	0.21	−0.91	0.14	0.01	0.09	0.13	−0.04	92.6%
DW_P	0.16	−0.11	−0.14	0.05	−0.88	0.06	−0.16	85.4%
UO_P	0.06	0.18	−0.75	0.09	−0.03	−0.23	−0.16	68.1%
TOX	−0.93	0.12	0.07	0.19	0.08	−0.17	0.17	98.0%

was varied, Fig. 6(b) is a similar plot showing the relationship between wafer-averaged X_3 values and threshold voltage adjust doses. Having interpreted the components any parameter can be represented as a linear combination of the named components. Ignoring a_{ij} coefficients with small magnitudes (< 0.1) we can represent the normalized n-channel 20/2-μm LAMBDA as

$$\text{LAMBDA\_N\_norm}$$
$$= 0.52X_{\Delta L} - 0.33X_{\Delta PWELL} + 0.52X_{\Delta XJ}. \quad (22)$$

Not surprisingly expression (22) suggests that the variation in this channel length modulation parameter depends on variations in channel length, P-well implant, and junction depths.

It is important to note that, as indicated by the final column of Table IV, not all of the variability of each individual model parameter can be recreated by the 7 chosen components. Thus when these components, and the a_{ij} coefficients contained in Table IV, are being employed to predict model parameter variations, allowances must be made to reintroduce any lost parameter variabilities. One solution to this problem would be to adjust the a_{ij} components to become

$$\frac{a_{ij}}{\sqrt{\dfrac{\text{var } P_i}{100}}}. \quad (23)$$

where var P_i is the percentage variance of parameter P_i which is accounted for by the 7 retained components as it appears for example in the last column of Table IV. This will result in the components being not strictly uncorrelated but any correlations introduced will be minor.

IV. WORST CASE MODEL GENERATION

The original set of 75 (3 geometries) correlated device model parameters has been effectively reduced to become a group of 7 uncorrelated process-related components by the transformations described in the previous section. The definition of worst case or statistical circuit design techniques in terms of these independent components is far easier to perform than if similar analyses had been derived for the original model parameters. The two main reasons for this simplification are firstly that troublesome correlations are eliminated and secondly the dimensionality of the problem can be considered to have been reduced from 75 to 7. The main purpose of this work has been to produce a framework for producing realistic worst-case model parameter sets from which device/circuit performance limits could be predicted accurately. Such a scheme will be detailed here. Relationships between the variabilities of the often empirical model parameters and variations in some core process parameters were also sought so as to allow for the possibility of linking device/circuit performance variabilities directly to these process parameters. Improvements in circuit yield brought about through the tightening of the controls of an identified process variable would be an obvious advantageous outcome of the derivation of such relationships. More rigorous statistical circuit analyses based on the manipulation of the independent components can also be an option, two such methods are briefly detailed.

B. Worst Case Analysis

In this analysis a set of component scores was generated corresponding to all possible combinations of the each of the 7 components set to $+/- 2.5$ (i.e., $+/- 2.5\sigma$ since
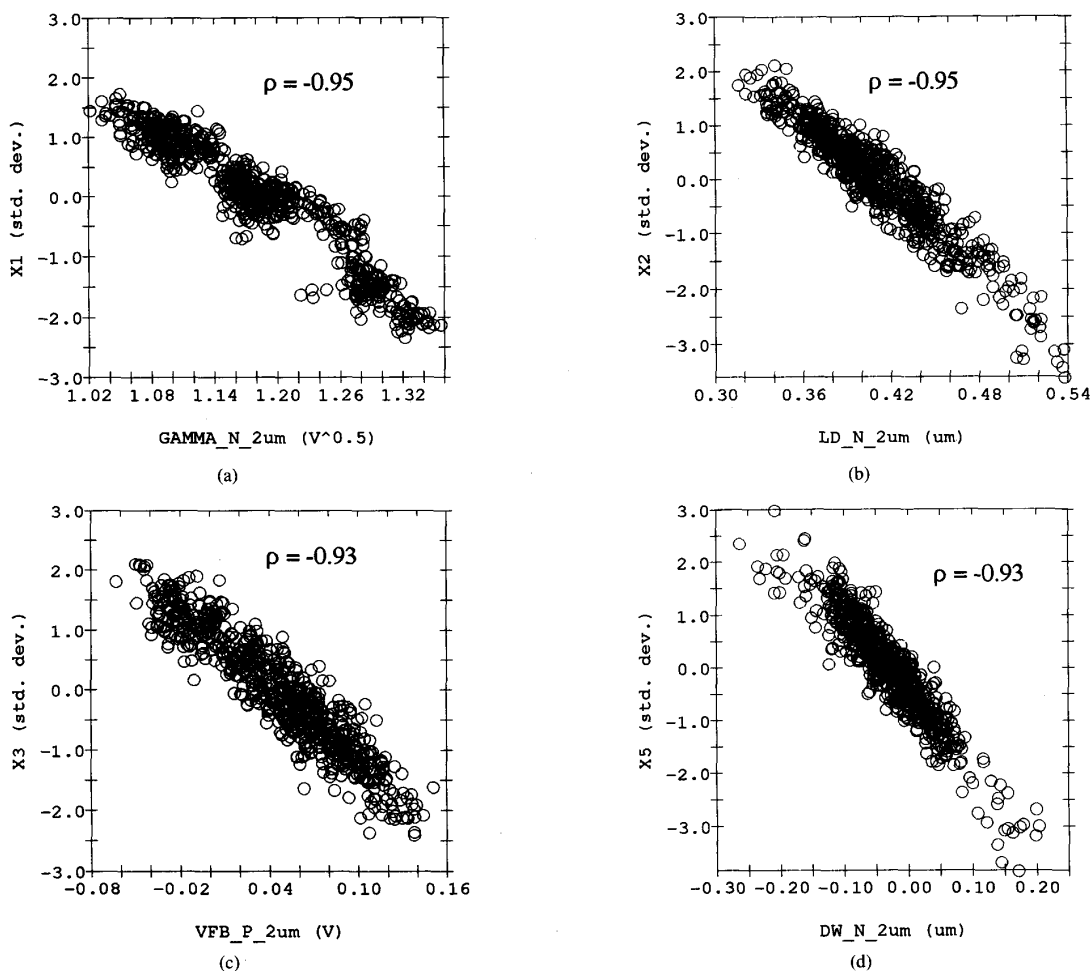
Fig. 5.   Scatter plots of components X_1, X_2, X_3, and X_5 versus the parameters with which they are highly correlated.

$\sigma = 1$ in this case). In all there were 2^7 (128) combinations of the 7 components. Next (19) and (23) are used to map the component scores onto 128 sets of normalized model parameter scores corresponding to 75 parameters each. The measured parameter means and standard deviations previously recorded are then utilized to denormalize the parameters. These 128 "corner" model parameter sets must now be reduced into a set of 2 "worst case" parameter sets. The following function is evaluated for each of the parameter sets

$$F(P) = \sum_{k=1}^{p} \left(\frac{B_1 I_{DSk}}{I_{DSnom}} + \frac{B_2 g_{dsk}}{g_{dsnom}} + \frac{B_3 g_{mk}}{g_{mnom}} \right). \quad (24)$$

In (24) B_1, B_2, and B_3 are weighting coefficients (usually 0 or 1), and the model equations are employed to calculate the I_{DS}, g_{ds}, and g_m simulated device characteristics at any of the p biases. The nominal characteristics in the denominators in (24) correspond to those simulated with the parameters set to their nominal values (i.e., X's = 0 in (19)). The parameter sets corresponding to the maximum and minimum instances of $F(P)$ are chosen to be the required two worst case parameter

sets. For the analysis of certain digital circuits B_2 and B_3 may be set to 0 and only one bias point for each device polarity (i.e., $p = 2$ where $V_{GS} = V_{DS} = +/ - 5$ V) may have been employed in the determination of the $F(P)$ values. Such a simplistic analysis may not be sufficient in analog applications where the device conductances and other device biasing arrangements can not be ignored. The worst case parameter sets generated in this work were aimed at analog applications, B_1 to B_3 were set to 1 and p was set to 10 (5 biases were considered adequate for both n-channel and p-channel 20/2-μm devices). The particular biases utilized included both low and high gate drives and involved the device being biased in both linear and saturation regions of operation. With the above conditions calculated $F(P)$ values would have a nominal value of 30 ($p = 10$ and $B_1 + B_2 + B_3 = 3$). The parameter sets associated with the maximum and minimum instances of $F(P)$ were deemed to be the required worst case parameter sets. In this experiment the maximum and minimum $F(P)$ values were approximately 50 and 17, respectively.

Certain device currents and conductances were recorded from each of the sites from which the initial parameter
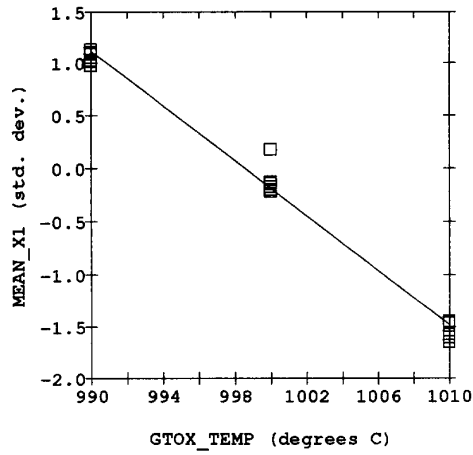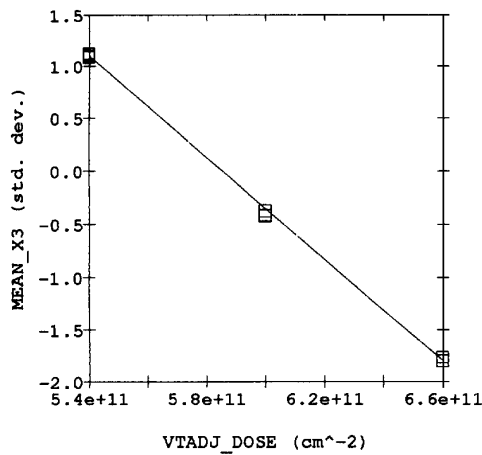
Fig. 6. (a) Wafer averaged X_1 values gate oxide temperature. (b) Wafer averaged X_3 values versus threshold voltage adjust dose.

extractions were performed. These device characteristics were then used to aid in the validation of the worst case parameter sets. Fig. 7 shows the measured distributions, and predicted nominal and worst case instances (wc_hi and wc_lo), of device current, output conductance, and transconductance for an n-channel 20/2-μm device biased at $V_{GS} = +3$ V, $V_{DS} = +4$ V and $V_{BS} = 0$ V. Fig. 8 shows similar information for a p-channel 20/2 μm device biased at $V_{GS} = -1.3$ V, $V_{DS} = -3$ V, and $V_{BS} = 0$ V. In both cases the simulated worst case bounds gave a very good indication of the actual range of operation for the device performances concerned. A comparison between the worst case models produced by the method reported in this document and a more traditional worst case analysis approach is possible by considering Fig. 9. This graph contains a measured histogram of measured transconductance for the p-channel 20/2-μm device biased at $V_{GS} = -3$ V, $V_{DS} = -4$ V, and $V_{BS} = +5$ V. The proposed upper and lower worst case limits (wc_hi and wc_lo), are again accurate while the other approach, where the individual parameters are set to $+/- 2.5\sigma$ limits so as to maximize and minimize
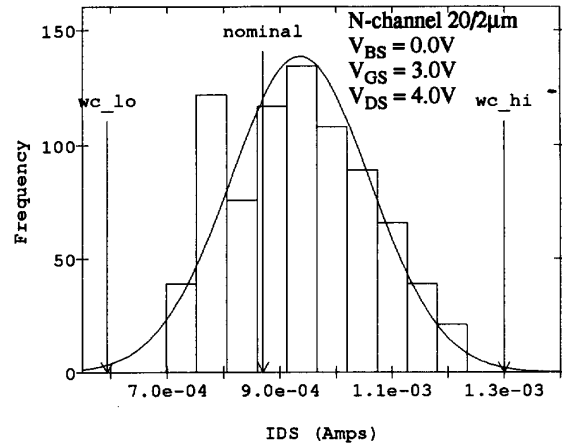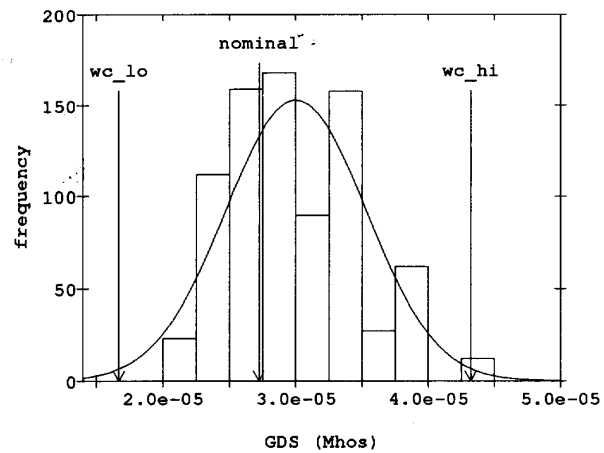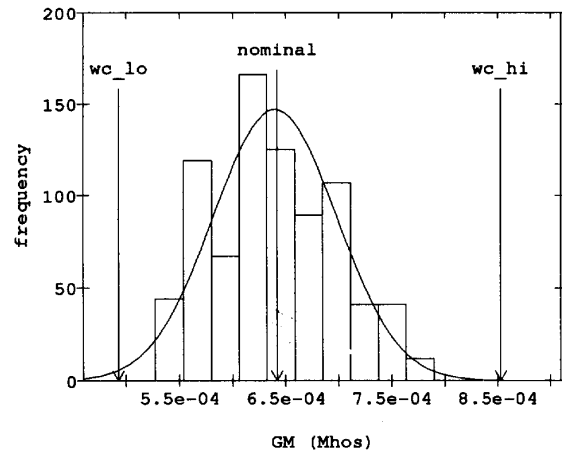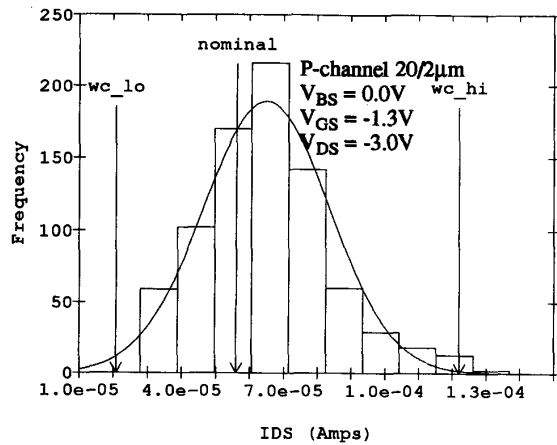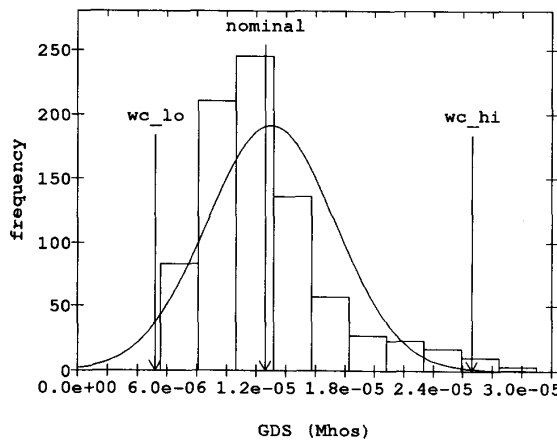

Fig. 7. Measured distributions of n-channel current, output conductance, and transconductance for the bias indicated with predicted nominal and worst case instances shown. (a) Current. (b) Output conductance. (c) Transconductance.
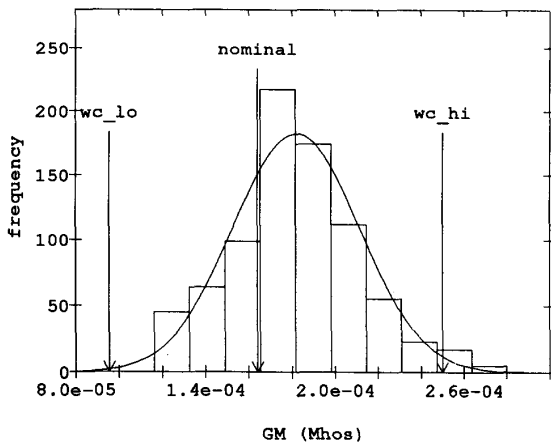
device current (wwc_hi and wwc_lo) are far too pessimistic because of the fact that parameter interdependencies were overlooked.

(a)

(b)

(c)

Fig. 8. Measured distributions of p-channel current, output conductance, and transconductance for the bias indicated with predicted nominal and worst case instances shown. (a) Current. (b) Output conductance. (c) Transconductance.

B. Correlated Monte Carlo Analysis

Another more rigorous way to predict the statistical spread in the performance of a particular device or circuit would be to perform a Monte Carlo analysis of the circuit under analysis and to examine the predicted performance distribution. This can be done by constructing parameter sets where the parameters are allowed to vary independent of one another (randomly) in accordance with their measured distributions. However, a Monte Carlo analysis of a device or circuit performance using these "random" model parameter sets can lead to inaccurate results [9], [10], and [26] because the parameter correlations are neglected. This problem can be overcome by randomly generating component sets (i.e., X's) and converting them to parameter sets, where measured parameter correlations are included, using (19). A Monte Carlo analysis in terms of these "correlated" parameter sets will be much more successful. The disadvantage of a Monte Carlo analysis is that the number of simulations required can be prohibitive in the case of large circuits. One hundred simulations [26] is often suggested as the minimum required in such an analysis. Fig. 10 shows measured and simulated distributions of drain current for 20/2-μm n-channel devices biased with $V_{GS} = V_{DS} = 5\,\text{V}$. Included among the simulated curves, scaled accordingly so as to appear with the measured data, are the results of performing Monte Carlo simulations employing 100 random and 100 correlated parameter sets. The correlated model parameter sets predicted a standard deviation of 221 μA which is in good agreement with the measured variation (240 μA). The random model parameter sets predicted a distribution with a standard deviation of 190 μA with the reduced accuracy being attributable to the exclusion of model parameter interdependencies. Random Monte Carlo analyses can lead to situations where the predicted performance distribution can be too tight (as in this case) or too loose depending on the correlations which exist between the model parameters to which this performance is sensitive [10].

C. Gradient Analysis

Another approach which has been proposed [7], [13] which leads to a more efficient prediction of a device/circuit performance spread is a methodology entailing a gradient or sensitivity analysis of the performance under examination (Z) and utilizing the factors identified by the PCA discussed earlier. The standard deviation in Z can be predicted using the following expression

$$\sigma_Z = \sqrt{\sum_{j=1}^{m}\left(\frac{\partial Z}{\partial X_j}\right)^2} \tag{25}$$

involving the gradients of the performance (Z) with respect to the process-related independent factors $(X$'s). Expression (25) is valid once the factors are uncorrelated and assuming that the relationship between the device/circuit performance and the factors can be approximated as being linear. The determination of σ_Z necessitates a minimum of $m+1$ simulations and since in this work we have defined 7 factors a total of 8 simulations are required to estimate the variance in any performance. This
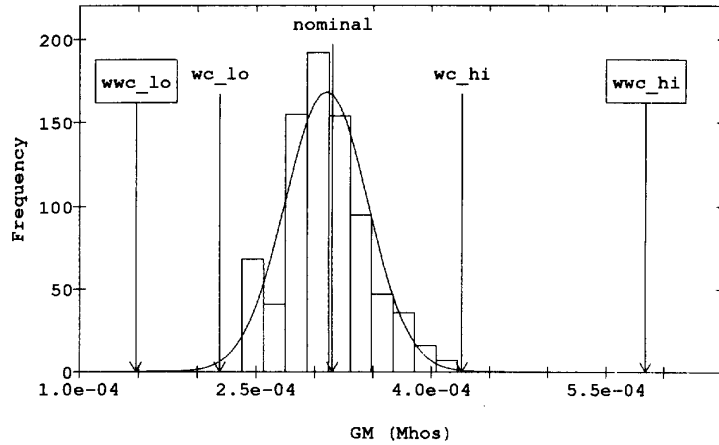
Fig. 9. Measured distribution of p-channel transconductance for a 20/2-μm p-channel device biased at $V_{BS} = 5\,V$, $V_{BS} = -3\,V$, and $V_{DS} = -4\,V$. The inner worst case limits are generated from the independent components and the outer worst case limits are generated utilizing the original parameter ignoring parameter correlations.

compares very favorably with the 100 or more simulations needed in the Monte Carlo analysis previously described to collect the corresponding information. Fig. 10 also includes a curve obtained with this methodology to predict the variability of the device current analyzed, the mean in this case was achieved by setting all device parameters to their mean values (i.e., X's = 0). The simulated performance variation (219 μA) is in very close agreement to the correlated Monte Carlo case but at a much reduced simulation cost (8 as opposed to 100). Parameter gradients or sensitivities could also have been utilized to perform a similar task. In (25)

$$\frac{\partial Z}{\partial X_j} = \sum_{i=1}^{n} \left(\frac{\partial Z}{\partial P_i} \cdot \frac{\partial P_i}{\partial X_j} \right) \tag{26}$$

where

$$\frac{\partial P_i}{\partial X_j} = a_{ij}. \tag{27}$$

If the circuit simulator in use has a parameter sensitivity analysis option then (25) to (27) can be combined to predict σ_Z so that the $m + 1$ simulations referred to by (25) do not have to be explicitly performed. The simulator would however require the information referred to in (27) as input.

V. CONCLUSIONS

An efficient methodology by which device model parameter variabilities and correlations can be related to the statistical process variations causing them has been developed and demonstrated. Statistical MOSFET parametric data from a CMOS process was gathered with the aid of specially formulated parameter extraction techniques employing analytical equation solving procedures. Multivariate statistical techniques including principal component analysis techniques were employed to convert the correlated model parameter set into a much smaller set of independent process-related factors. Worst case and more robust statistical circuit evaluation techniques, constructed utilizing these uncorrelated factors, have
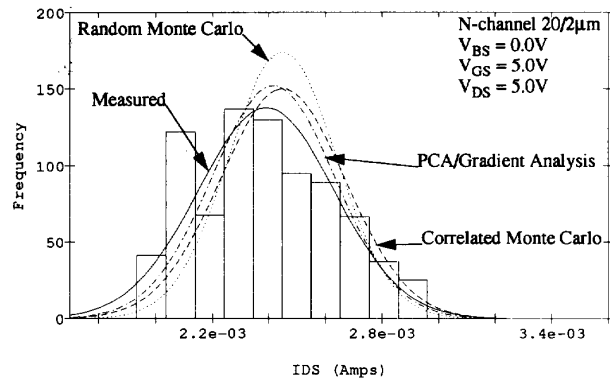

Fig. 10. Measured distribution of n-channel current at the bias indicated with predicted distributions also shown.

been detailed. These techniques are far simpler and more easily implemented than techniques performed utilizing the original model parameters because troublesome correlations are avoided and there are far less process-related factors than model parameters leading to a reduction in the dimensionality of the problem. Measured variations in device currents and conductances have been employed to validate the accuracy of various procedures which have been proposed. Furthermore, important relationships were determined between the empirical but readily measured model parameters and the underlying process variabilities which may not be so easy to monitor. Thus, vital links have been identified between the CAD model parameters used by circuit designers and the process-related variables understood by the process engineers. This in turn enables the possibility of circuit yield improvements by tightening the control on certain process variables isolated by the analysis and also identifying those process variables for which less or reduced control is required, thus reducing process complexity and widening process windows.

REFERENCES

[1] L. Maliniak, "Engineers must make manufacturing a priority," *Electron. Des.*, pp. 39–48, Oct. 15, 1992.

[2] P. Yang, D. Hocevar, P. Cox, C. Machala, and P. Chatterjee, "An integrated and efficient approach for MOS VLSI statistical circuit design," *IEEE Trans. Computer-Aided Des.*, vol. CAD-5, no. 1, pp. 5–14, Jan 1986.

[3] N. Herr and J. J. Barnes, "Statistical circuit simulation modeling of CMOS VLSI," *IEEE Trans. Computer-Aided Des.*, vol. CAD-5, no. 1, pp. 15–22, Jan. 1986.

[4] S. R. Nassif, A. J. Strojwas, and S. W. Director, "A methodology for worst-case analysis of integrated circuits," *IEEE Trans. Computer-Aided Des.*, vol. CAD-5, pp. 104–113, Jan. 1986.

[5] T. K. Yu, S. M. Kang, I. N. Hajj, and T. N. Trick, "Statistical performance modeling and parametric yield estimation of MOS VLSI," *IEEE Trans. Computer-Aided Des.*, vol. CAD-6, no. 6, pp. 1013–1022, Nov. 1987.

[6] C. K. Chow, "Projection of circuit performance distributions by multi-variate statistics," *IEEE Trans. Semicond. Manufact.*, vol. 2, no. 2, pp. 60–65, May 1989.

[7] M. Bolt, M. Rocchi, and J. Engel, "Realistic statistical worst-case simulations of VLSI circuits," *IEEE Trans. Semicond. Manufact.*, vol. 4, no. 3, pp. 193–198, Aug. 1991.

[8] I. C. Kizilyalli, T. E. Ham, K. Singhal, J. W. Kearney, W. Lin, and M. J. Thoma, "Predictive worst case statistical modeling of 0.8-μm BICMOS bipolar transistors: A methodology based on process and mixed device/circuit level simulations," *IEEE Trans. Electron Devices*, vol. 40, no. 5, pp. 966–973, May 1993.

[9] S. Inohira, T. Shinmi, M. Nagata, T. Toyabe, and K. Iida, "A statistical model including parameter matching for analog integrated circuits simulation," *IEEE Trans. Computer-Aided Des.*, vol. CAD-4, no. 4, pp. 621–628, Oct. 1985.

[10] J. A. Power, A. Mathewson, and W. A. Lane, "MOSFET statistical parameter extraction using multivariate statistics," in *Proc. IEEE ICTMS'91*, vol. 4, pp. 209–214, Mar. 1991.

[11] J. A. Power, A. Mathewson, and W. A. Lane, "An approach for relating model parameter variabilities to process fluctuations," in *Proc. IEEE ICTMS'93*, vol. 6, pp. 63–68, Mar. 1993.

[12] C. Michael and M. Ismail, "Statistical modeling of device mismatch for analog MOS integrated circuits," *IEEE J. Solid-State Circuits*, vol. 27, no. 2, pp. 154–165, Feb. 1992.

[13] J. A. Power, D. Barry, A. Mathewson, and W. A. Lane, "Accurate and efficient predictions of statistical circuit performance spreads," in *Proc. IEEE CICC'92*, pp. 3.3.1–3.3.4, May 1992.

[14] J. A. Power and W. A. Lane, "An enhanced SPICE MOSFET model suitable for analog applications," *IEEE Trans. Computer-Aided Des.*, vol. CAD-11, no. 11, pp. 1418–1425, Nov. 1992.

[15] Y. Tsividis and K. Suyama, "MOSFET modeling for analog circuit CAD: Problems and prospects," in *Proc. IEEE CICC'93*, pp. 14.1.1–14.1.6, May 1993.

[16] D. E. Ward and K. Doganis, "Optimized extraction of MOS model parameters," *IEEE Trans. Computer-Aided Des.*, vol. CAD-1, no. 4, pp. 163–168, Oct. 1982.

[17] P. Yang and P. K. Chatterjee, "An optimal parameter extraction program for MOSFET models," *IEEE Trans. Electron Devices*, vol. ED-30, no. 9, pp. 1214–1218, Sept. 1983.

[18] P. Conway, C. Cahill, W. A. Lane, and S. U. Lidholm, "Extraction of MOSFET parameters using the simplex direct search optimization method," *IEEE Trans. Computer-Aided Des.*, vol. CAD-4, no. 4, pp. 694–698, Oct. 1985.

[19] M. F. Hamer, "First-order parameter extraction on enhancement silicon MOS transistors," in *IEE Proc.*, vol. 133, pt. I, no. 2, pp. 49–54, Apr. 1986.

[20] H. P. Tuinhout, S. Swaving, and J. J. M. Joosten, "A fully analyt-ical MOSFET model parameter extraction approach," in *Proc. IEEE ICTMS'88*, vol. 1, pp. 79–84, Feb. 1988.

[21] J. A. Power and W. A. Lane, "Enhanced SPICE MOSFET model for analog applications including parameter extraction schemes," in *Proc. IEEE ICTMS'90*, vol. 3, pp. 129–134, Mar. 1990.

[22] G. T. Wright, "A simple and continuous MOSFET model," *IEEE Trans. Electron Devices*, vol. ED-32, no. 7, pp. 1259–1263, July 1985.

[23] B. J. Sheu, D. L. Scharfetter, P. K. Ko, and M. C. Jeng, "BSIM: Berkeley short-channel IGFET model for MOS transistors," *IEEE J. Solid-State Circuits*, vol. 22, no. 2, pp. 558–565, Aug. 1987.

[24] J. E. Jackson, *A User's Guide To Principal Components.* New York: Wiley-Interscience, 1991.

[25] R. J. Harris, *A Primer of Multivariate Statistics*, 2nd Ed. Orlando, FL: Academic Press, 1985.

[26] C. K. Chow, "Statistical circuit simulation of a wideband amplifier: A case study in design for manufacturability," *Hewlett-Packard J.*, pp. 78–81, Oct. 1990.

James A. Power (M'89) received the B.E., M.Eng.Sc., and Ph.D. degrees in microelectronics degrees from University College Cork, Ireland, in 1986, 1988, and 1992, respectively.

From 1986 to 1993 he was a Research Scientist at the National Microelec-tronics Research Centre, Cork, Ireland, where his responsibilities included device modeling, device test, parameter extraction, and developing statistical circuit design methodologies. Since 1993 he has been with SILVACO Data Systems in Santa Clara, CA, where he is currently Division Manager for Device Characterization. His current research interests include parameter extraction techniques, device modeling for circuit simulation, statistical circuit design, and statistical process control.

Brian Donnellan received the B.Eng. (Electronic) from the University of Limerick, Ireland, in 1985.

He joined Analog Devices B.V., Limerick, Ireland, in 1985 as a De-vice Modeling Engineer and is now CAD Manager responsible for device modeling, design entry, circuit simulation, behavioural modeling, and lay-out generation at Analog Device's Limerick Design and Manufacturing centre. His special interests include statistical simulation and Design-For-Manufacturability.

Alan Mathewson graduated from the Polytechnic of Newcastle upon Tyne (U.K.).

In 1978 he worked for Plessey Research Caswell and Racal Advanced Development Division on as-pects of silicon CMOS and bipolar technologies.

In 1982 he joined the National Microelectronics Research Centre (NMRC) in Ireland as a Research Scientist, where he was involved in the start-up phase of the NMRC and participated in the devel-opment of processes for the development of their first CMOS Technologies. Subsequently, he was involved in the development and characterization of all new processes in the NMRC and in 1993 he was made Silicon Research Group Director responsible for the coordination of research activities in the materials and device characterization area. He is coauthor of approximately 60 papers on aspects of silicon technology nonvolatile memory and device modeling. His main research interests include applications of EEPROM technology, silicon device characterization, and integrated sensors.

Mr. Mathewson is also a member of the Electro Chemical Society and SPIE—The Society For Optical Engineering.

William A. Lane received the B.A.Sc. and M.A.Sc. degrees from the University of Toronto, Toronto, Canada, in 1977 and 1980, respectively, and the Ph.D. degree from the National University of Ireland in 1987.

From 1980 to 1987 he was employed at the National Microelectronics Research Centre, University College, Cork, Ireland, where he was engaged in IC process and device research and development and in analytical device modelling and characterisation with a special interest in analogue compatible models. In 1987 he joined Analog Devices B.V. as Process Development Manager and was responsible for the development of several mixed signal BiCMOS processes. Since 1990, while maintaining the Analog Devices link, he is now back with the NMRC, responsible for silicon technology. He has published over 40 papers in silicon technology and CAD modeling areas.